Hierarchical upconversion nanocomposite materials containing lanthanide-doped nanoparticles

Ying Bao[§], Chaoyang Jiang[*]

Department of Chemistry, University of South Dakota, Vermillion, South Dakota 57069, USA
[§]Present address: Department of Chemistry and The James Franck Institute, The University of Chicago, Chicago, Illinois 60637, USA

[*]Author for correspondence: Chaoyang Jiang, email: Chaoyang.Jiang@usd.edu
Received 6 Aug 2013; Accepted 26 Aug 2013; Available Online 26 Aug 2013

Abstract

Upconversion nanocomposite materials have received increasing interest in both fundamental researches and practical applications. Lanthanide-doped nanoparticles, integrated in a variety of hierarchical nanocomposite materials, exhibit unique nonlinear optical property, which convert low energy photons into higher energy radiation. Upconversion nanocomposite materials may be utilized in various fields, such plasmon enhanced fluorescence, security technique and anti-counterfeiting materials, biomedical imaging, and photovoltaic devices. This review summarizes some recent progresses regarding the upconversion nanocomposites and their applications, and provides opinions on the challenges in this subject for future applications.

Keywords: Lanthanide-doped nanoparticles; Upconversion nanoparticles; Hierarchical nanocomposite

1. Introduction

Upconversion (UC) nanocomposite materials are a group of nanocomposites that emit high-energy photons in visible or ultraviolet regions with successive absorption of two or more low energy photons typically in the near infrared (NIR) regions [1]. Lanthanide-doped nanoparticles are one of the most active types of components in the upconversion nanocomposites due to the existence of multiple metastable energy levels in lanthanide ions which are critical for efficient UC processes. The increasing active research of lanthanide-doped UC nanoparticles (UCNPs) has resulted in numerous publications from a large number of research groups, as well as several review articles, covering a broad range of topics such as chemical syntheses [2,3], surface modification [4,5], assembly [6], and applications in bioconjugation, biomedical imaging [7], and cancer therapy [8-10]. Some upconversion composite nanostructures were also discussed in a review article with a focus on biomedical applications [9]. As we will demonstrate below, there are extensive studies conducted on upconversion nanocomposite materials. These UC nanocomposites have been widely applied in fields of plasmon enhanced fluorescence, security technique and anti-counterfeiting materials, biomedical imaging, and photovoltaic devices. In this review paper, we will summarize some recent progress regarding the designs, fabrications and applications of UC nanocomposites, and provide our opinions on the challenges in studying such UC nanocomposite materials.

1.1. UCNP synthesis and UC mechanisms

Lanthanide doped UCNPs are one type of unique material in the family of UC nanomaterials, which also involves lanthanum phosphate nanostructures [11], rare earth ions in glass [12], and others [13]. Lanthanide doped nanoparticles typically includes one or more types of lanthanide ions in an inorganic host matrix [14-16]. To facilitate efficient UC process, the host matrix must have low lattice photon energies and high chemical stability. Ideal host materials include fluorides (such as $NaYF_4$, KYF_4, LaF_3, and YF_3) and oxides (such as ZrO_2 and Y_2O_3). The UC efficiency of UCNPs can be largely impacted by the crystallinity of host materials and size, chemical composition and surface state of nanocrystals [17,18].

Depending on the various host matrices, UCNPs can be synthesized via co-precipitation method, thermal decomposition method, hydrothermal method, sol-gel process, and others. There are several review articles that provided detailed discussion on those synthetic methods [1,2,6]. To facilitate the applications of UCNPs, particularly in the fields of biomedical imaging, there are increasing efforts to synthesize sub-10 nm nanoparticles without sacrificing their UC efficiencies. For example, Han and co-workers presented a simple thermolysis method to prepare lanthanide-doped YF_3 nanocrystals with a diameter of 3.7 nm, and they found that the UC intensity was ten times brighter than CaF_2 nanocrystals (4.5 nm) [19]. Cohen and co-workers reported the successful syntheses of beta-phase $NaYF_4$:20% Yb^{3+}, 2% Er^{3+} nanocrystals with controlled diameters from 4.5 to 15 nm [20]. In their work, experimental conditions, such as concentration of basic surfactants, ratio of Y^{3+} and F^- ions, and temperature, were modulated to tune the size of the UC nanocrystals (Figure 1). Milliron and co-workers demonstrated the usage of an automated platform for the reproducible synthesis of lanthanide-doped $NaYF_4$ nanoparticles with controlled crystal phase and maximum upconversion luminescence *via* thermal decomposition [21].

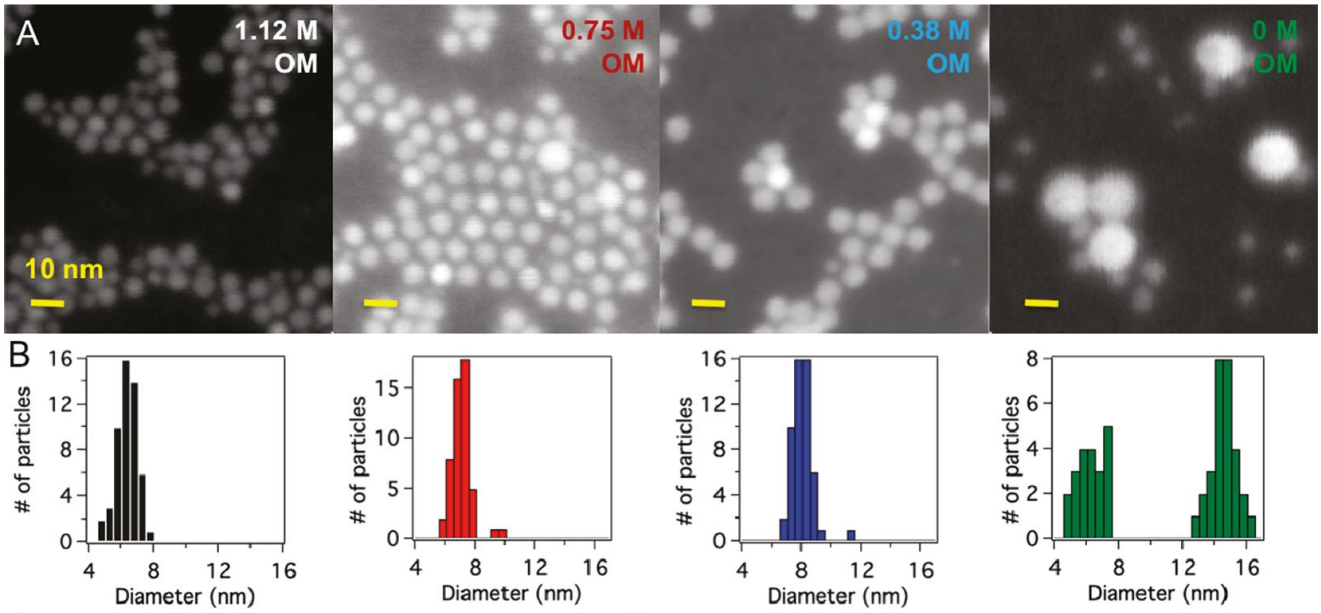

Figure 1. (A) Scanning transmission electron microscopy (STEM) images of representative β-$NaYF_4$ nanoparticle samples at different oleylamine concentrations of 1.12, 0.75, 0.38, and 0 M. Scale bar in each image is 10 nm. (B) Nanocrystal size distributions, measured by TEM (n = 50 for each). (Adapted from Ref. 20 with permission. Copyright 2012, American Chemical Society).

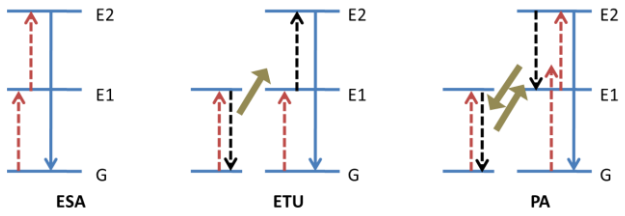

Figure 2. Three types of upconversion process, excited state absorption (ESA), energy transfer upconversion (ETU), and photon avalanche (PA).

The UC process is a nonlinear optical process that can involve several energy states and steps of energy transfers. Very briefly, there are three types of UC processes: excited state absorption (ESA), energy transfer upconversion (ETU), and photon avalanche (PA). As shown in Figure 2, every UC mechanism is related to a simple three-level energy system: ground level (G), metastable excited level (E1), and higher excited level (E2). In the ESA case, ground state absorption (GSA) will be followed by a second photon absorption, which promotes the lanthanide ions from E1 to E2. Then UC emission will release a high energy photon, corresponding to the E2 to G optical transition. The ETU process starts with a same GSA step and then an energy transfer from a neighboring ion causes the ion into the E2 level. PA mechanism is an unusual UC mechanism that only occurs with high intensity excitation. Among these three mechanisms, the ETU is a main mechanism for many co-doped UCNPs and the UC efficiency is closely related to the concentration of co-doped ions (inter-ion distances) and their relative ratios. Yb^{3+} ions are often used as energy donors (sensitizer) due to their simple energy level diagram (around 980 nm absorption with $^2F_{7/2}$ to $^2F_{5/2}$ transition). The energy from Yb^{3+} will transfer to neighboring emitting ions (activator) for an efficient UC emission. A typical ratio of 10 is used for sensitizer vs. activator that will facilitate the sufficient energy transfer and minimize non-radiative processes such as cross-relaxation energy loss.

1.2. UC nanocomposites

UC nanocomposites typically contain several types of nanoscale building blocks and matrix materials with at least one kind of UCNPs as the UC component. The integration of UCNPs into nanocomposite materials has significantly expanded the application fields of UC materials. In order to have strong chemical bonds or other interactions between the UCNPs and matrix materials, proper chemical modifications are designed to alternate the surface properties of the upconversion nanoparticles, including hydrophilicity, chemical affinity, stability, and functionality. Furthermore, a variety of approaches have been developed recently to integrate the surface modified UCNPs into hierarchical UC nanocomposites with well controlled structure and functionality.

Surface modifications on UC nanoparticles play a critical role in preparing the UC nanocomposite materials, due to the organic ligands capping on most of the as-synthesized UCNPs. Overall, current methods for surface modification can be classified into two categories: modification of existing ligands and coating of additional materials. The modification of existing ligands can be either ligand exchange or ligand reaction. For example, sodium citrate was used to convert oleic acid-caped $NaYF_4$: Yb, Er UCNPs into hydrophilic ones using a solution-based ligand exchange process [22]. The resulting citrate-caped UCNPs have a zeta potential of -50.8 mV, which make these products suitable in layer-by-layer (LbL) assembly of nanocomposite multilayer thin films. Surface modification with poly(acrylic acid) (PAA) on UCNPs was also successfully demonstrated [23-26]. Example of ligand oxidation can be the products of carboxyl groups from the carbon-carbon double bonds of oleic acid with Lemieux-von Rudloff reagent, another unique method to convert hydrophobic UCNPs into hydrophilic ones [27,28]. Several other methods have been developed as well to coat additional materials on the surface of UCNPs, such as of LbL assembly,

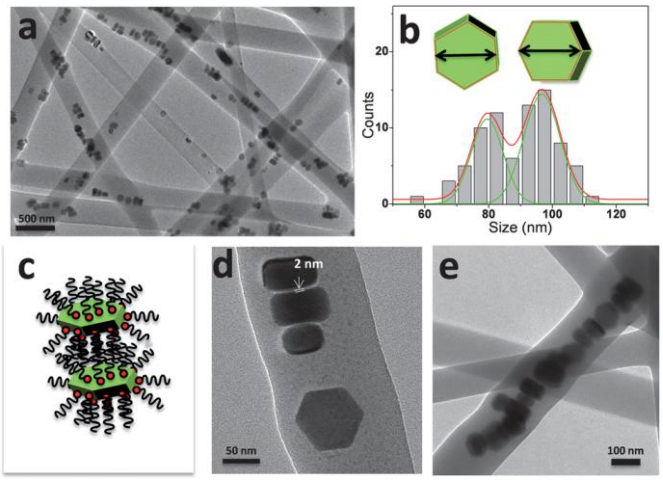

Figure 3. (a) TEM micrograph of UCNP/PMMA nanofibers; (b) size distribution of UCNPs; (inset: hexagonal plate of UCNPs); (c) schematic representation of two face-to-face aligned oleic acid-capped UCNPs; (d and e) high magnification TEM images of UCNP/PMMA nanofibers. (Reproduced from Ref. 36 with permission from The Royal Society of Chemistry).

host-guest interaction, and attachment of amphiphilic polymers and other functional materials. For example, Budijono et al. produced block-copolymer protected UCNPs via flash nano-precipitation (FNP) method [29]. In their work, block-copolymers were used for the FNP-coated UCNPs and these UCNPs are stable in buffers and serum media. Such FNP modification not only promotes the study of UCNPs in bioimaging and photodynamic therapy, but also facilities the integration of functional nanocomposites. Another example of surface modification is in a study of stem cell labeling where covalently conjugated UCNPs are much more stable than those with conventional electrostatic LbL assembly for better labeling and tracking [30].

Integration of the surface modified UCNPs into UC nanocomposites with well-controlled structures and functionalities can be achieved by various approaches, such as polymer encapsulation [31], in-situ polymerization [32], silica coating and functionalization [33-35], electrospinning [36-41], LbL assembly [22,42-44], and direct writing and screen printing [45]. For example, Liu and co-workers encapsulated UCNPs together with iron oxide nanoparticles via a microemulsion method [31]. They first dissolved poly(styrene-block-allyl alcohol) in chloroform with UCNPs and iron oxide nanoparticles, then added the organic solution into an aqueous solution of polyvinyl alcohol for the microemulsion process [31]. On the other hand, Zhang et al. synthesized raspberry-like polystyrene/UCNP nanocomposites via an in situ dispersion polymerization technique [32]. Besides polymer, silica coating is also widely applied on UCNPs for a variety of applications. Huang and co-workers prepared a multimodal luminescent probe by capping silica-coated UCNPs with fluorescein isothiocyanante (FITC) [33]. To attach gold colloids, Fuji and co-workers used 3-aminopropyltrimethoxy silane to functionalize the silica shell of UCNPs and they utilized the silica shell to separate the UCNPs and the metal shells [35]. LbL assembly can also be used to attach gold nanoparticles onto UCNPs [42,43]. Bao et al. demonstrated a fabrication of polymer/UCNP multilayer thin films via LbL assembly and found that the UCNPs were uniformly distributed in the multilayer thin films [22]. Wang et al. synthesized manganese-doped UCNPs with multiple layers of Chlorin e6 and increase in vitro photodynamic therapy efficacy was observed [44]. UCNP nanofibrous composites can be prepared using electrospinning polymer spin-dope containing UCNPs [36-41]. Bao and co-workers found that the UCNPs in fibrous nanocomposite formed chain-like aggregates aligned along the fiber axes (Figure 3). The authors believed that such alignments can be originated from the assembly of UCNP plates and the dynamic process in the electrospinning procedure. There is only a slight reduction of UC efficiency for the UCNPs in electrospun nanofibers [36]. Another method to prepare UC nanocomposites is using patterned direct-write and screen printing of UC inks, which were recently reported by several groups [45-48]. Kellar and co-workers used composite ink containing UCNPs in their direct writing, and they found that it is critical to tune the parameters of both ink preparations and printing procedures for the overall performance optimizations [45].

1.3. Manipulation of UC in nanocomposites

Upconversion luminescence is one of the most important properties for hierarchical UC nanocomposites. The UC efficiency of nanocomposite materials can be either quenched, controlled modulated, preserved, or enhanced, depending on the purpose of the nanocomposites, the design of the nanocomposite structures, and the interaction with the other functional components in the nanocomposites.

UC quenching sometime happens when the active components in nanocomposites interfere the stability of the meta-stable states of the lanthanide ions. The surface quenching effect can be quite severe especially when the size of UCNPs is reduced. Liu and co-workers conducted a systematic spectroscopic investigation on $NaGdF_4$ UCNPs with various sizes [49]. Furthermore, they compared the two types of UCNPs: with and without a protection layer, which was synthesized through an epitaxial growth method. Their results indicated that the variation in UCNP size has extremely limited effect on the UC emission, thus providing direct evidence on the surface quenching effect and the size-dependent UC luminescence. The organic and polymer matrix in nanocomposite materials usually can cause some UC quenching effect due to the photon-relaxation of the organic molecules. With careful design of the UC nanocomposites, such UC quenching can be well-controlled so that the UC property of the fabricated nanocomposites can be preserved

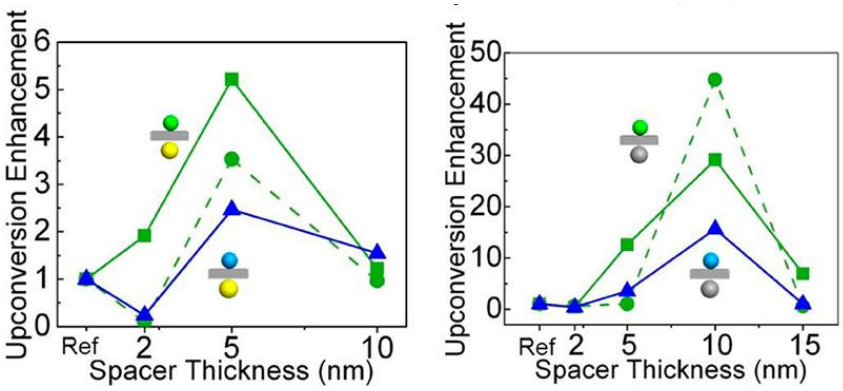

Figure 4. Integrated area under the peak as a function of the Al_2O_3 layer thickness normalized to that of the pure UCNP sample for (left) Au NPs and (right) Ag NPs.(Adapted with permission from Ref. 52. Copyright 2012, American Chemical Society).

[22,36]. UC quenching can also occur when UCNPs in the nanocomposites are interacted with metal shells [35,50]. Fujii and co-workers recently studied UC properties of nanocomposites consisting of lanthanide-doped $NaYF_4$ cores and gold shells. Combined with experimental photoluminescence data and theoretical calculation, the authors studied the impact mechanism of gold shells on the UC photoluminescence [35].

On the other hand, research activities on the enhancement of upconversion in the nanocomposite materials are more intensive than those of UC quenching. In most of the UC enhancement studies, active components in the nanocomposites are typically metallic nanostructures, which have unique plasmonic properties and can optically interact with UCNPs [35,42,51-53]. Both gold nanoparticles and amorphous gold shells were utilized in enhancing the UC luminescence of UCNPs in the nanocomposites. Duan and co-workers modulated UC emission through plasmonic interactions between the UCNPs and gold nanoparticles [42]. Surface-plasmon-coupled emission was proposed in their work and the increase of radiative decay rate was observed. The authors also found that the formation of gold shell can suppress the emission due to light scattering [42]. Kennedy and co-workers studied the metal-enhanced UC luminescence on cubic phase lanthanide-doped $NaYF_4$ crystals [51]. In their work, an enhancement factor of 2-8 was reported, depending on the emission peaks and the UCNP compositions [51]. The mechanism of enhancement and quenching of UC luminescence was further explored theoretically and experimentally by Fuji and co-workers. They concluded that a structure of dielectric core with a metal shell is a promising system for plasmon-induced UC enhancements [35]. Kagan and co-workers demonstrated the UC enhancement of hexagonal $NaYF_4$ doped with lanthanide dopants by close proximity to metal nanoparticles [52]. They found the UC enhancements are up to 5.2 fold proximal to gold nanoparticles and of up to 45 fold proximal to silver nanoparticles (Figure 4). The UC enhancements can be originated from both resonant plasmonic coupling and nonresonant near-field enhancement from the metal nanoparticle [52]. Kim and co-workers obtained a 27-fold enhancement on gold nanorod-decorated UCNPs, and they revealed a 1 pM detection limit for biomolecules by using the gold nanorod-enhanced UC luminescence [54]. By using polyamidoamine generation 1 dendrimer as spacer, they coated gold and silver nanoshells on UCNPs and observed significant and selective enhancement (over 20 fold) of green, violet, and blue emission [54].

2. Nanocomposites with various geometries

The assembly of functional nanocomposites by integrating upconversion nanomaterials with other useful materials has obtained much attention due to their great potential for broad applications [33]. Based on the final geometry and structure of the nanocomposites, we here classify the upconversion nanocomposites into following types: zero-dimensional core-shell nanospheres, one-dimensional nanofibers, two-dimensional nanoscale thin films, and three-dimensional hieratical nanostructures.

2.1. Zero-dimensional core-shell nanospheres

Core-shell structures of UCNPs are often designed to protect and enhance the UC luminescent property, in which a shell of material is coated around the UC nanoparticles [55]. For the case of hydrophilic UCNPs, the core-shell structure can separate the UCNPs with the surrounding environments such as aqueous solution, which often leads to quench UC luminescence. In core-shell UC nanostructures, materials such as gold, silver, silica, tinania, and even UC host materials are widely used to form a shell with controlled thickness and porosity surrounding UCNP cores.

UCNP host materials can be used as special materials in preparing core-shell nanocomposites. For example, Mai et al. fabricated a core/shell UCNP structure with $NaYF_4$ as an inert shell [17]. They demonstrated that the shell formation can greatly enhance green emission. This is due to the fact that shell for UCNPs could dramatically decrease the surface defects and surface ligands influence and thus decrease the associated nonradiative decays [17]. Similarly, active shell doped with lanthanide ions was also fabricated on the surface of UCNPs. Vetrone et al. reported the fabrication of core-shell structure for $NaGdF_4$:Er^{3+}, Yb^{3+} nanoparticles and demonstrated that the luminescent intensity changes with different shell coatings [55]. In their results, the active-core $NaGdF_4$: Er^{3+}, Yb^{3+}/active–shell $NaGdF_4$: Yb^{3+} nanoparticles have stronger luminescent intensity compared to the active-core $NaGdF_4$: Er^{3+}, Yb^{3+}/inert–shell $NaGdF_4$ (see Figure 5). The enhancement of UC intensity is attributed to the active-shell, which helps to protect the luminescing Er^{3+} ions from the non-radiative decay as well as to transfer NIR absorbed radiation to the luminescing core [55]. Zhang and co-workers

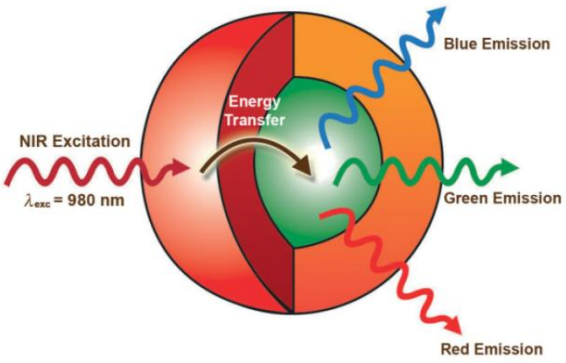

Figure 5. General depiction of the active-core/active-shell nanoparticle architecture showing the absorption of NIR light by the Yb^{3+}-rich shell (represented in red) and subsequent energy transfer to the Er^{3+}/Yb^{3+} co-doped core (represented in green), which leads to upconverted blue, green, and red emissions. (Reprinted with permission from Ref. 55. Copyright 2009, Wiley-VCH Verlag GmbH & Co. KGaA).

recently reported a successive layer-by-layer strategy and prepared core-shell structures via multi-shell epitaxial growth [56]. In their work, core-shell UCNPs with well-controlled shell thickness (0.36 nm per monolayer) were demonstrated by simply tuning the amounts of the shell precursors and they found that UC core-shell nanoparticles exhibited more stable UC emission in resisting the water quenching [56].

Oxide materials are also utilized as shell materials to form UC core-shell nanostructures. Due to the broad biological applications of UCNPs, silica, which is biologically and chemically stable, becomes an attractive option to fabricate the shell of UCNPs [57]. Li and co-workers coated uniform silica on $NaYF_4$:Yb,Er nanospheres and produced multicolor UC nanospheres based on a fluorescence resonance energy transfer (FRET) mechanism [57]. Yang et al. demonstrated a strategy to fabricate core/shell structured nanocomposites with LaF_3:Yb^{3+},Er^{3+} nanoparticle cores and mesoporous silica shells [34]. Furthermore, they have demonstrated that the mesoporous silica shells not only have less effect on luminescence intensity, but also allow the confinement and control of the diffusion of molecules, which can be used in drug delivery. The silica shells also facilitate the anchoring of biomolecules onto the UCNPs due to well-developed approaches in attaching biomolecules on silica surface [58]. On the other hand, tinania shells are integrated onto UC core-shell nanoparticles. Tang and co-workers recently synthesized such nanoparticles with a two-step chemical synthesis [59]. They found that the core-shell nanoparticles exhibited interesting photocatalytic activity under NIR irradiation and the degradation of organic molecules was caused mostly by the oxidation of oxygen species from a photocatalytic reaction [59].

Metallic nanomaterials have been fabricated as shells on the surface of UCNPs to affect emission intensity of UCNPs due to their unique plasmonic properties [35,51,60]. Kannan et al. have prepared a type of UCNP nanocomposite by selective growth of gold and silver nanoshells [61]. In their study, the Au and Ag nanoshells grew on dendrimer functionalized UCNPs which resulted in a significant enhancement of emission intensity from the UC nanocomposites [61]. Lately, the same group published another study about the use of an assembly of gold nanorods to decorate UCNPs and the enhancement in UC luminescence for such UCNP nanocomposites was found to be 11.2 fold [54]. While the metal materials can enhance the excitation and emission, they also can quench the emission due to the energy transfer. Zhang et al. prepared UCNPs decorated with either gold nanoparticles or continuous gold nanoshells [42]. They demonstrated that the emission intensity of UCNPs is largely dependent on the morphology of the gold nanostructures. The UC emission can be enhanced with gold nanoparticle coating and will be quenched with continuous Au nanoshells [42]. Dong and co-workers prepared UCNP/Ag core-shell structures and studied their unique bio-functional properties [62]. With the silver shell coating, the authors found that cancer cells were killed with 980 nm illumination and the cytotoxicity of the composite nanoparticles was reduced as compared to the raw UCNPs [62].

Polymer encapsulated UCNPs are another type of zero-dimensional UC core-shell nanocomposites [31,32,63]. Several approaches, such as in situ polymerization and polymer wrapping, can be utilized to prepare polymer encapsulated UC nanocomposites. Zhang and co-workers synthesized nanocomposite spheres containing polystyrene and upconversion nanoparticles via an in situ dispersion polymerization technique [32]. Moreover, with an amphiphilic block copolymer, it was able to encapsulate hydrophobic UCNPs with other functional nanomaterials. Xu et al. fabricated an UCNP/iron oxide nanoparticle@polymer nanocomposite system via a microemulsion method [31]. Such nanocomposites, due to their multi-functionality, could be further used to load dye molecules or drugs for multimodal biomedical imaging and cancer therapy.

2.2. One-dimensional nanofibers

UC composite nanofibers are one-dimensional nanostructures containing functional nanoscale components possessing unique UC properties. Compared to spherical core-shell structures, UC nanofibers represented more complicate nanostructures in preparations, properties, and applications. Electrospinning technique has been used in preparing UC nanofibers with various matrix materials, UC nanofillers, and functionalities [39]. UC nanofibers, together with other nanostructures (such as nanorods [64-66], nanowires [67,68], and nanotubes [69]), are the essential parts of one-dimensional UC nanomaterials, which has great potentials in various applications such as solar cell, biosensing, and bioimaging.

Polymer, due to its easy functionality, versatility, and robustness, is a common matrix for incorporating UCNPs and other functional nanomaterials into nanofibers. Bao et al. has directly fabricated oleic acid coated UCNPs into poly(methyl methacrylate) (PMMA) nanofibers using electrospinning technique [36]. After integrated into polymeric nanofibers, the UCNPs with well-preserved UC properties can be observed from the composite nanofibrous films and even individual nanofibers (see Figure 6). Polyvinylpyrrolidone (PVP) can also be used as polymer matrix in fabricating UC nanofibers via electrospinning technique [70,71]. Both research groups have observed the increase of UC emission for PVP/UCNP nanofibers and the detail mechanisms were discussed.

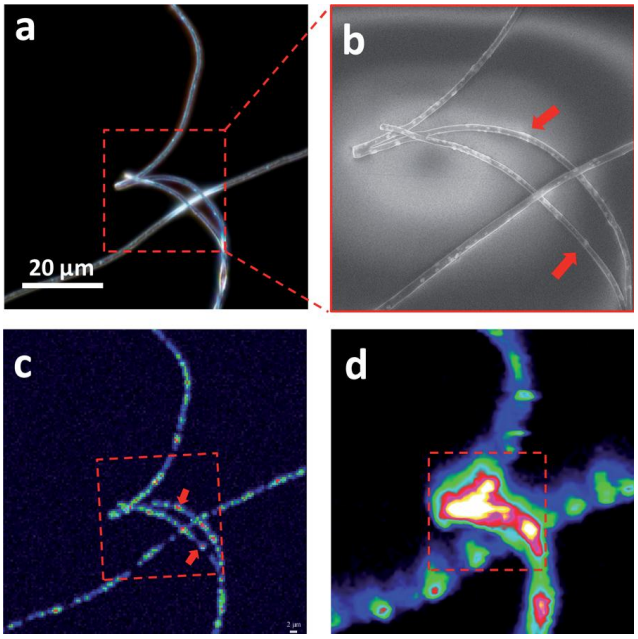

Figure 6. (a) Dark field optical image of several individual UCNP/PMMA nanofibers; (b) SEM image of the area of interest shown in (a); (c) confocal luminescence mapping image excited with 532 nm; and (d) confocal upconversion mapping excited with 980 nm. (Reproduced from Ref. 36 with permission from The Royal Society of Chemistry).

Furthermore, UCNPs also can be fabricated into one-dimensional nanofibers with a variety of inorganic materials, such as metallic material, semiconductor, and silica. Dong et al. have demonstrated that the luminescent intensity of UCNP/PVP nanofibers decreases gradually with the addition of embedding Ag nanoparticles [37]. Ji et al. prepared UCNP supported TiO_2 nanobelts which demonstrated very strong UC emission [72]. Silica is another popular inorganic material used for integrating UCNPs due to its well-known biocompatibility. Several papers were published on the fabrication and property study of electrospun UC luminescence porous $NaYF_4$@silica fibers [73,74]. Hou et al. reported a study on drug-delivery properties of an electrospun UC luminescence porous $NaYF_4$@silica fiber [74,75]. In their study, the porous structure can be obtained after annealing the precursor nanofibers (Figure 7). The resulting nanocomposites possess both porous structure and UC properties which were used as host carriers for drug delivery applications.

2.3. Two-dimensional nanoscale thin films

Another well-studied UC nanocomposite was two-dimensional thin films. Uniformly incorporating UCNPs into thin films has been proposed in a broad range of materials and devices for various applications. Recently, there has been increasing interests on the fabrications of UC thin films by various methods such as spin coating [52,76-78], solution coating [79], dip coating [80], LbL assembly [22] and in-situ growth [81].

For the UC thin films fabricated by spin coating method, Paudel et al. spun coated the UC thin films onto designed substrates and studied the UC luminescence enhancement [76]. In their study, the substrates were designed into engineering plasmonic surface, consisting of gold nanopillars on continuous gold films with their surface plasmon resonance coupled to the NIR excitation wavelength

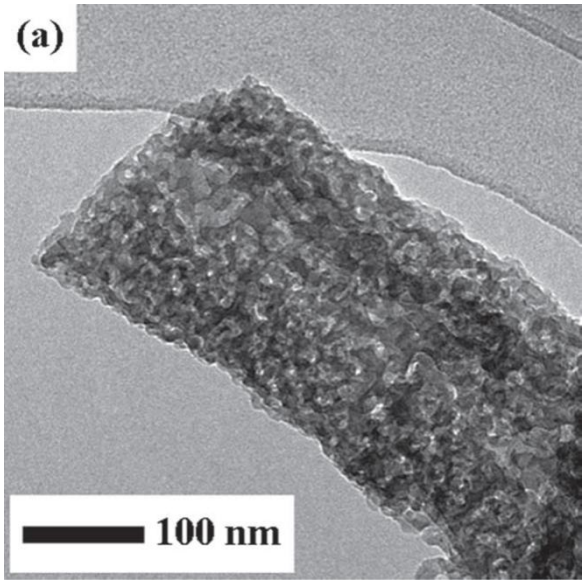

Figure 7. TEM image of $NaYF_4$:Yb^{3+}, Er^{3+}@silica fibers. (Adapted with permission from Ref. 74. Copyright 2011, Wiley-VCH Verlag GmbH & Co. KGaA).

[76]. TEM results showed that the UC thin films prepared with spin coating method contain high density UCNPs without significant aggregations. The significant enhancement of UC emission was observed from their thin film nanocomposites [76]. Similarly, Saboktakin et al. spun coated UC thin films on a dense layer of silver or gold NPs and studied the effects on their UC emission intensity [52]. Sol-gel method was used in preparing UC nano films [77,78]. Sivakumar et al. reported a silica sol-gel UC thin film by combining sol-gel method and spin coating approach and a new UC process was discussed [77]. Furthermore, Wu et al. coated UCNPs on thin films of cross-linked liquid crystal polymers and observed fast bending of the films upon exposure to NIR light at 980 nm [79]. (Figure 8) Bao et al. have fabricated freestanding upconversion multilayer thin films by combining ligand exchange process and LbL assembly [22]. The resulted UC thin films containing homogeneously distributed UCNPs demonstrated strong mechanical robustness and well-preserved UC properties [22]. Yan and co-workers presented a prototype of rewritable two-dimensional optical storage medium with potential high-density recording capacity [82]. They modulated UC nanopatterns by a photochromic diarylethene and found that near-IR excitation for reading the UC emission is a nondestructive process. Three methods, spin-coating, the Langmuir-Blodgett assembly, and evaporation-induced self-assembly, were utilized and compared in preparing the composite UC thin films [82].

2.4. Three-dimensional nanostructures

Polymeric upconversion nanocomposites with three-dimensional structures are another important group of UC nanocomposites in order to advance the development of UC materials for wide applications. Similar to other multi-dimensional nanostructures, the interaction between the UCNPs and other building blocks plays an essential role in determining the properties of the final nanocomposites. UC three-dimensional nanostructures can be fabricated with a variety of approaches, such as in-situ polymerization [83], sol-

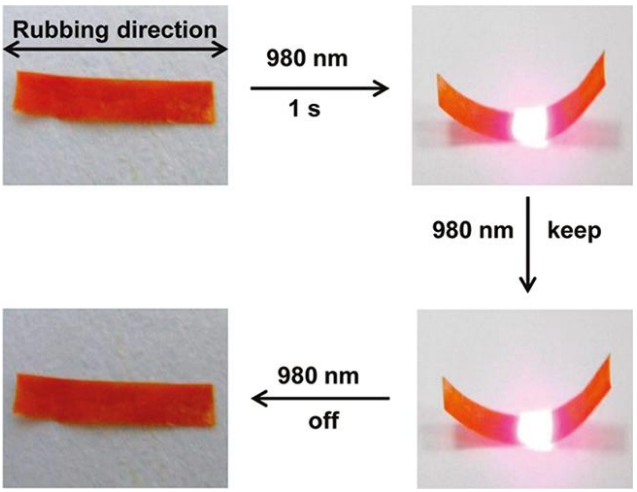

Figure 8. Photographs of the azotolane CLCP/UCNP composite film bending toward the light source along the alignment direction of themesogens, remaining bent in response to the CW NIR irradiation at 980 nm (power density = 15 W/cm^2), and becoming flat again after the light source was removed. The size of the composite film was 8 mm×2 mm×20 μm. (Reprinted with permission from Ref. 79. Copyright 2011, American Chemical Society).

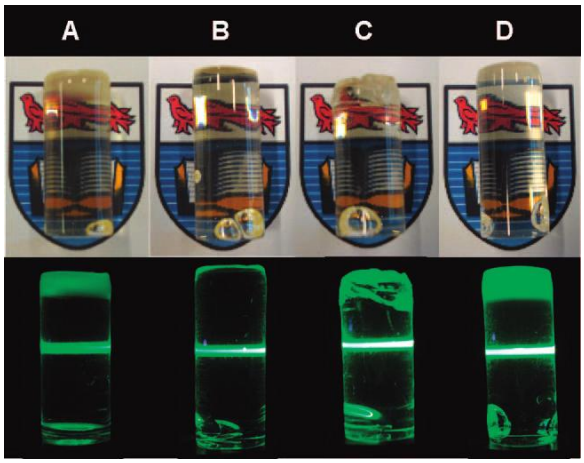

Figure 9. Photographs of NP-PMMA composites under ambient light (top) and 980 nm laser diode excitation (bottom) (A) 0.5 wt %, (B) 1 wt %, (C) 2 wt %, and (D) 3 wt % $NaYF_4$:2% Er^{3+}, 20% Yb^{3+} NPs in PMMA. (Reprinted with permission from Ref. 83. Copyright 2009, American Chemical Society).

gel method [84,85], direct-write printing [45,47], self-assembly [86], and successive absorption [87].

Recently, a fabrication of bulk UC polymeric nanocomposites was reported [83]. Boyer et al. presented an in-situ polymerization method to fabricate UC particle polymer composites [83]. In their work, the bulk polymer composites are transparent and their UC properties are well preserved. (Figure 9) The ability of preparing transparent bulk polymer composites can facilitate the 3D volumetric optical display. Similarly, Tan et al. reported the fabrications of transparent infrared-emitting nanocomposites of UCNP with PMMA and polystyrene (PS) for optical applications [88]. May and co-workers have fabricated large UC monoliths without high temperature treatment [89]. The same group has reported the fabrication of patterned upconversion inks for direct-write printing and security applications [45]. The upconversion ink, prepared by well suspending UCNPs in PMMA toluene solution, requests no post-processing and can be printed in various substrates such as glass, silicon and paper [45]. Quick Response (QR) codes made of UCNP inks have been demonstrated [47]. Furthermore, the UCNPs can be encapsulated into microporous metal-organic framework (MOF) materials, as being reported by Huo group [87]. In their strategy, UCNPs were successively absorbed into the forming surfaces of the growing MOF crystals [87]. The hybrid UCNP/MOF composites exhibit the identical emission wavelength which is originated from the non-encapsulated UCNPs [87]. Recently, nanocomposites containing graphenes and UCNPs were reported and their unique properties have demonstrated great potential for various applications [81,90,91].

3. Applications

Upconversion nanocomposites with a variety of shapes and structures have unique UC properties, from which visible emissions can be obtained upon the excitation of near infrared excitations. Such optical properties allow the application of the UC nanocomposites in various fields, such as security printings, solar cells, biomedical imaging, and cancer therapy.

3.1. Security printing

Application of UC nanocomposites in security printing and anti-counterfeiting technique is growing very fast in recent years because of the easy syntheses of high efficient UCNPs and the development of assembly methods for nanocomposites. Prasad and co-workers prepared photopatternable $NaYF_4$ UCNPs via a ligand exchange process and fabricated films with multilayer color-coded patterning [46]. The films can easily emit visible photons upon the excitation with the low-power, inexpensive invisible NIR laser, which indicates their great potential in anti-counterfeit marks [46]. Patterned direct-write and screen printing of UC inks were recently reported by Kellar and co-workers [45]. The authors described the direct-write printing of high-resolution polymer features containing UCNPs for security applications. UCNPs embedded in the poly(methyl methacrylate) were $NaYF_4$: Er, Yb which are capped with oleic acid. The UC features were deposited successfully onto a variety of substrates including high bond paper, Kapton, and glass, and they are invisible to the naked eye [45]. The same research team also reported the development of quick response codes (Figure 10) using an AutoCAD file on Optomec direct-write aerosol jetting [47]. The UC QR codes can not only be scanned for information sharing application, it can also be used for security purpose [47]. Current work is focused on the optimization of ink formulations for better mechanical stability and color control.

3.2. Solar cells and light harvesting

Lanthanide materials have a long history of being used to convert photons to different wavelengths which can be more useful in applications [92]. The usage of lanthanide-doped UCNPs and their composites can convert low energy photons into high energy photons that can be absorbed by the solar cells, thus reduce the so-called spectral mismatch and improve the cell efficiency [90-94]. In 1996, the first demonstration of UC-enhanced solar cells was done with a

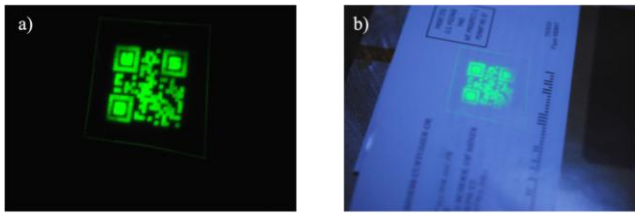

Figure 10. (a) Upconversion image of the covert QR code on a transparent tape. (b) Upconversion image of the QR code on transparent tape affixed to the label of a magazine. (Reprinted with permission from Ref. 47. Copyright 2012, IOP Publishing).

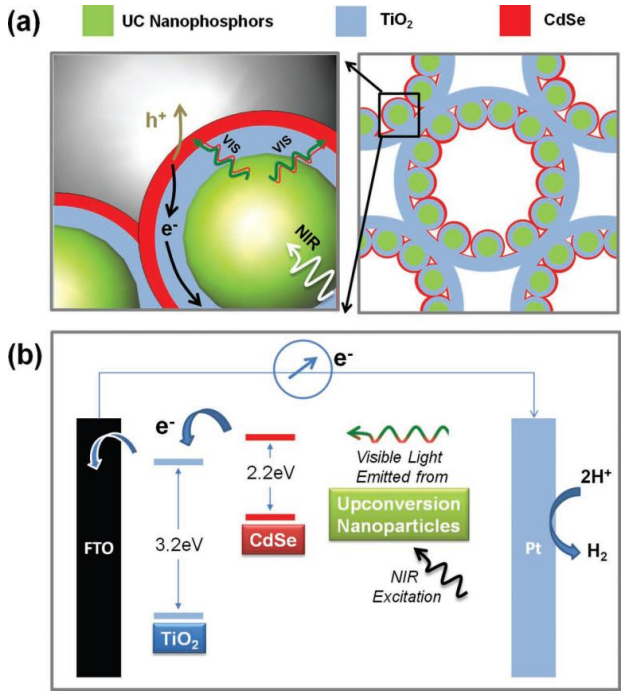

Figure 11. a) Schematic of energy flow in the as-prepared hetero-nanostructures from upconversion nanoparticles to visible light-absorbing CdSe nanoparticles to TiO_2 Inverse Opals upon near-infrared photoexcitation. b) Energy diagram illustrating the charge injection from the excited CdSe into TiO_2 and the transport of photoinjected electrons to the electrode surface for hydrogen generation. (Reprinted with permission from Ref. 98. Copyright 2013, Wiley-VCH Verlag GmbH & Co. KGaA).

GaAs cell and a quadratic dependence on incident light intensity was observed [95]. Atre and co-workers used numerical techniques and demonstrated the enhancement of UC efficiency in solar cells using plasmonic nanostructures [96]. They obtained an over 10-fold absorption enhancement for sub-bandgap radiation and a 100-fold increase in above-bandgap power emission toward the active components in solar cells [96]. Demopoulos applied UCNPs with the shape of dexagonal nanoplates as an external layer in dye-sensitized solar cells and approximately 10% improvement in photocurrent and energy efficiency was observed [97]. Su et al. recently designed an interconnected porous network and enhanced near-infrared light harvesting [98]. In their work, titanium oxide inverse opal was used to efficiently load the UCNPs and quantum dot sensitizers. The energy flow in the solar cells is shown in Figure 11 where UCNPs are the starting points for light harvesting. With the high UCNP loading and the strong light scattering in the hierarchical porous network, the authors successfully demonstrated hydrogen generation via a photoelectrochemical process using near-infrared irradiation [98]. Photocatalytic degradation of organic dyes on UCNP/TiO_2 nanocomposites under solar light irradiation was also demonstrated [84].

3.3. Biomedical application

Upconversion nanomaterials are widely utilized in biomedical imaging, drug delivery, and phototherapy [99]. This is due to their unique properties, including easy syntheses, high degree of photostability, a high efficiency, low excitation energy that is less harmful to biomolecules [51]. With the fast development in this field, there are several excellent reviews focused on biomedical applications of UC nanomaterials, including nanocomposite materials [4,100,101].

UC nanocomposite materials with unique upconversion properties demonstrated promising applications in biomolecular imaging [102-105]. For example, Chen and co-workers prepared biocompatible core/shell UCNPs with high efficient NIR-to-NIR upconversion. Exceptional image contrast (S/N of 310) was obtained and UC luminescence imaging of deep tissue was demonstrated (see Figure 12) [104]. Furthermore, dual functional UCNPs were developed to facilitate the dual imaging techniques [31,102,103]. Liu and co-workers encapsulated UCNPs together with iron oxide nanoparticles via a microemulsion method. They found that drug molecules can be further loaded inside the nanocomposites for imaging-guided and magnetic targeted drug delivery [31]. Another example of the multifunctional UCNPs is the preparation of UCNPs with both UC luminescence and superparamagnetic properties for guided stem cell therapy [103]. In their work, ultrahigh tracking sensitivity with a detection limit of 10 cells was reported [103].

UC nanocomposites are also widely used in controlled drug delivery [34,63,74] and photodynamic therapy [44,62,106-108]. Zhang et al. prepared mesoporous silica nanocomposites with LaF_3:Yb, Er cores [34]. With the unique mesoporous structure, the confinement and control diffusion of molecules can be achieved, thus allowing their potential application in drug delivery systems [34]. Similarly, Lin and co-workers fabricated UCNP-decorated silica nanofibers using electrospinning process [74]. The authors also investigated drug storage/release properties using ibuprofen as a model drug. They found that the UC luminescence intensity increases with the cumulative released drug molecules, which is due to the quench effect caused by adsorbed ibuprofen molecules [74]. UCNP nanocomposites can also be ideal candidates for photodynamic therapy (PDT) because they can be easily excited with low cost NIR diode lasers at a wavelength for relative deep penetration in tissues. For example, Shan and co-workers prepared pegylated UCNP nanocomposites containing meso-tetraphenylporphine (TPP) and studied their PDT behavior [107]. Qian et al. utilized gold decorated core/shell/shell upconversion nanocomposites in their study of efficiently photothermal destruction of BE(2)-C neuroblastoma cells [108]. Wang and co-workers recently reported the syntheses of manganese doped UCNPs with a charge-reversible property and studied their imaging-guided pH-sensitive PDT under near-infrared light [44]. In their work, LbL assembly was used to load activate Chlrin e6 conjugated polymers onto UCNPs in order to generate singlet oxygen ($^1O_2$) to kill cancer cells. Their results confirmed that UC

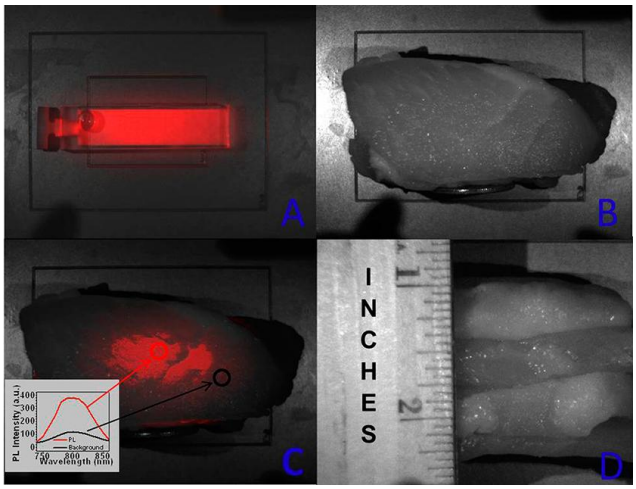

Figure 12. (a) UCPL bright-field image of a cuvette filled with a suspension of the core/shell nanoparticles, (b) bright-field image of a cuvette covered with pork tissue with a quarter coin stood aside showing its thickness, (c) merged UCPL/bright-field image of the cuvette covered with pork tissue, and (d) bright-field image of the pork tissue (side view). The inset in (c) shows the spectra obtained from the circled areas. (Reprinted with permission from Ref. 104. Copyright 2012, American Chemical Society).

nanocomposite with designed surface functionality can serve as smart pH-responsive PDT agent in cancer theranostics [44].

4. Conclusion and Outlook

In conclusion, we have discussed a variety of hierarchical upconversion nanocomposite materials, ranging from syntheses and surface modification of upconversion nanoparticles, to the interaction between the UCNPs and other components. We have presented several types of nanocomposite materials, based on their overall shape and morphology, including core-shell nanoparticles, one-dimensional nanofibers, two-dimensional thin films, and three-dimensional nanostructures. The applications of these UC nanocomposites in the fields of security printing, solar cells and light harvesting, biomedical imaging, drug delivery, and photo dynamic therapy were briefly introduced.

Overall, upconversion nanocomposite materials have demonstrated enormous potential for broad applications in fields such as energy, security, and biomedicine. There are several technique challenges in the development of upconversion nanocomposites. First, it is necessary to continue exploring novel approaches in preparing UC nanocomposites with well-designed nanostructures and interaction within the nanocomposites. Second, further improve the upconversion efficiency for the UC nanocomposite, particularly with small UCNPs. This also includes the design of new plasmon-enhanced UC nanocomposites. Next, investigate the interaction between the UC nanocomposites and their environments, including proper surface functionality of the nanocomposites, optical, mechanical, electrical, interaction of UC nanocomposites with other components in solar cells, and also chemical and biological interactions of the UC nanocomposite with biomolecules, cells, and tissues. Last, but not least, explore new functionalities for UC nanocomposite materials and discover new application fields, especially for multifunctional nanocomposite materials.

References

1. M. Haase, H. Schafer, Angew. Chem. Int. Ed. 50 (2011) 5808.
2. F. Wang, X. G. Liu, Chem. Soc. Rev. 38 (2009) 976.
3. J. Chen, J. X. Zhao, Sensors 12 (2012) 2414.
4. M. Wang, G. Abbineni, A. Clevenger, C. B. Mao, S. K. Xu, Nanomed-Nanotechnol 7 (2011) 710.
5. C. Li, J. Lin, J. Mater. Chem. 20 (2010) 6831.
6. D. Vennerberg, Z. Lin, Sci. Adv. Mater. 3 (2011) 26.
7. H. S. Mader, P. Kele, S. M. Saleh, O. S. Wolfbeis, Curr. Opin. Chem. Biol. 14 (2010) 582.
8. C. Wang, L. Cheng, Z. Liu, Theranostics 3 (2013) 317.
9. L. Cheng, C. Wang, Z. Liu, Nanoscale 5 (2013) 23.
10. G. Han, G. Y. Chen, Theranostics 3 (2013) 354.
11. L. Xu, H. W. Song, B. A. Dong, Y. Wang, X. Bai, G. L. Wang, Q. Liu, J. Phys. Chem. C 113 (2009) 9609.
12. F. Pelle, F. Auzel, J. Alloys Compd. 300 (2000) 131.
13. W. Deng, D. Y. Jin, K. Drozdowicz-Tomsia, J. L. Yuan, J. Wu, E. M. Goldys, Adv. Mater. 23 (2011) 4649.
14. Y. Wu, X. Shen, S. X. Dai, Y. S. Xu, F. F. Chen, C. G. Lin, T. F. Xu, Q. H. Nie, J. Phys. Chem. C 115 (2011) 25040.
15. F. Wang, X. G. Liu, J. Am. Chem. Soc. 130 (2008) 5642.
16. H. Na, K. Woo, K. Lim, H. S. Jang, Nanoscale 5 (2013) 4242.
17. H. X. Mai, Y. W. Zhang, L. D. Sun, C. H. Yan, J. Phys. Chem. C 111 (2007) 13721.
18. M. C. Tan, L. Al-Baroudi, R. E. Riman, ACS Appl. Mater. Interfaces 3 (2011) 3910.
19. G. Y. Chen, H. L. Qiu, R. W. Fan, S. W. Hao, S. Tan, C. H. Yang, G. Han, J. Mater. Chem. 22 (2012) 20190.
20. A. D. Ostrowski, E. M. Chan, D. J. Gargas, E. M. Katz, G. Han, P. J. Schuck, D. J. Milliron, B. E. Cohen, ACS Nano 6 (2012) 2686.
21. E. M. Chan, C. X. Xu, A. W. Mao, G. Han, J. S. Owen, B. E. Cohen, D. J. Milliron, Nano Lett. 10 (2010) 1874.
22. Y. Bao, Q. A. N. Luu, C. Lin, J. M. Schloss, P. S. May, C. Jiang, J. Mater. Chem. 20 (2010) 8356.
23. T. Konishi, K. Shimizu, Y. Saito, K. Saga, J. Photopolym. Sci. Technol. 20 (2007) 11.
24. L. Wang, Y. Zhang, Y. Zhu, Nano Res. 3 (2010) 317.
25. X. Kang, D. Yang, Y. Dai, M. Shang, Z. Cheng, X. Zhang, H. Lian, P. a. Ma, J. Lin, Nanoscale 5 (2013) 253.
26. L. Xiong, T. Yang, Y. Yang, C. Xu, F. Li, Biomaterials 31 (2010) 7078.
27. Z. Chen, H. Chen, H. Hu, M. Yu, F. Li, Q. Zhang, Z. Zhou, T. Yi, C. Huang, J. Am. Chem. Soc. 130 (2008) 3023.
28. G. Wang, Q. Peng, Y. Li, J. Am. Chem. Soc. 131 (2009) 14200.
29. S. J. Budijono, J. Shan, N. Yao, Y. Miura, T. Hoye, R. H. Austin, Y. Ju, R. K. Prud'homme, Chem. Mater. 22 (2010) 311.
30. L. Zhao, A. Kutikov, J. Shen, C. Y. Duan, J. Song, G. Han, Theranostics 3 (2013) 249.
31. H. Xu, L. Cheng, C. Wang, X. X. Ma, Y. G. Li, Z. Liu, Biomaterials 32 (2011) 9364.
32. X. Y. Zhang, Y. Ren, M. Chen, L. M. Wu, J. Colloid Interface Sci. 358 (2011) 347.
33. H. Hu, L. Q. Xiong, J. Zhou, F. Y. Li, T. Y. Cao, C. H. Huang, Chem-Eur. J. 15 (2009) 3577.
34. Y. F. Yang, Y. Q. Qu, J. W. Zhao, Q. H. Zeng, Y. Y. Ran, Q. B. Zhang, X. G. Kong, H. Zhang, Eur. J. Inorg. Chem. 2010 (2010) 5195.
35. M. Fujii, T. Nakano, K. Imakita, S. Hayashi, J. Phys. Chem. C 117 (2013) 1113.
36. Y. Bao, Q. A. N. Luu, Y. Zhao, H. Fong, P. S. May, C. Jiang, Nanoscale 4 (2012) 7369.
37. G. P. Dong, X. F. Liu, X. D. Xiao, B. Qian, J. Ruan, S. Ye, H. C. Yang, D. P. Chen, J. R. Qiu, Nanotechnology 20 (2009) 055707.
38. G. P. Dong, X. F. Liu, X. D. Xiao, B. Qian, J. Ruan, H. C. Yang, S. Ye, D. P. Chen, J. R. Qiu, IEEE Photonic Tech L. 21 (2009) 57.

39. R. Y. Yang, G. S. Qin, D. Zhao, K. Z. Zheng, W. P. Qin, J. Fluorine Chem. 140 (2012) 38.
40. R. Y. Yang, W. Y. Song, S. S. Liu, W. P. Qin, CrystEngComm 14 (2012) 7895.
41. D. Li, W. S. Yu, X. T. Dong, J. X. Wang, G. X. Liu, J. Fluorine Chem. 145 (2013) 70.
42. H. Zhang, Y. Li, I. A. Ivanov, Y. Qu, Y. Huang, X. Duan, Angew. Chem. Int. Ed. 49 (2010) 2865.
43. L. Y. Wang, R. X. Yan, Z. Y. Hao, L. Wang, J. H. Zeng, H. Bao, X. Wang, Q. Peng, Y. D. Li, Angew. Chem. Int. Ed. 44 (2005) 6054.
44. C. Wang, L. Cheng, Y. M. Liu, X. J. Wang, X. X. Ma, Z. Y. Deng, Y. G. Li, Z. Liu, Adv. Funct. Mater. 23 (2013) 3077.
45. T. Blumenthal, J. Meruga, P. S. May, J. Kellar, W. Cross, K. Ankireddy, S. Vunnam, Q. N. Luu, Nanotechnology 23 (2012) 185305.
46. W. J. Kim, M. Nyk, P. N. Prasad, Nanotechnology 20 (2009) 185301.
47. J. M. Meruga, W. M. Cross, P. S. May, Q. Luu, G. A. Crawford, J. J. Kellar, Nanotechnology 23 (2012) 395201.
48. A. Bednarkiewicz, D. Wawrzynczyk, A. Gagor, L. Kepinski, M. Kurnatowska, L. Krajczyk, M. Nyk, M. Samoc, W. Strek, Nanotechnology 23 (2012) 145705.
49. F. Wang, J. A. Wang, X. G. Liu, Angew. Chem. Int. Ed. 49 (2010) 7456.
50. J. Sun, H. P. Liu, D. Wu, B. Dong, L. K. Sun, Mater. Chem. Phys. 137 (2013) 1021.
51. L. Sudheendra, V. Ortalan, S. Dey, N. D. Browning, I. M. Kennedy, Chem. Mater. 23 (2011) 2987.
52. M. Saboktakin, X. C. Ye, S. J. Oh, S. H. Hong, A. T. Fafarman, U. K. Chettiar, N. Engheta, C. B. Murray, C. R. Kagan, ACS Nano 6 (2012) 8758.
53. P. Zhao, Y. H. Zhu, X. L. Yang, K. C. Fan, J. H. Shen, C. Z. Li, RSC Adv. 2 (2012) 10592.
54. P. Kannan, F. A. Rahim, R. Chen, X. Teng, L. Huang, H. D. Sun, D. H. Kim, ACS Appl. Mater. Interfaces 5 (2013) 3508.
55. F. Vetrone, R. Naccache, V. Mahalingam, C. G. Morgan, J. A. Capobianco, Adv. Funct. Mater. 19 (2009) 2924.
56. X. M. Li, D. K. Shen, J. P. Yang, C. Yao, R. C. Che, F. Zhang, D. Y. Zhao, Chem. Mater. 25 (2013) 106.
57. Z. Q. Li, Y. Zhang, S. Jiang, Adv. Mater. 20 (2008) 4765.
58. T. J. Yoon, K. N. Yu, E. Kim, J. S. Kim, B. G. Kim, S. H. Yun, B. H. Sohn, M. H. Cho, J. K. Lee, S. B. Park, Small 2 (2006) 209.
59. Y. N. Tang, W. H. Di, X. S. Zhai, R. Y. Yang, W. P. Qin, ACS Catalysis 3 (2013) 405.
60. W. Deng, L. Sudheendra, J. B. Zhao, J. X. Fu, D. Y. Jin, I. M. Kennedy, E. M. Goldys, Nanotechnology 22 (2011) 325604.
61. P. Kannan, F. A. Rahim, X. Teng, R. Chen, H. D. Sun, L. Huang, D. H. Kim, RSC Adv. 3 (2013) 7718.
62. B. A. Dong, S. Xu, J. A. Sun, S. Bi, D. Li, X. Bai, Y. Wang, L. P. Wang, H. W. Song, J. Mater. Chem. 21 (2011) 6193.
63. B. Ungun, R. K. Prud'homme, S. J. Budijono, J. N. Shan, S. F. Lim, Y. G. Ju, R. Austin, Opt. Express 17 (2009) 80.
64. L.-N. Sun, H. Peng, M. I. J. Stich, D. Achatz, O. S. Wolfbeis, Chem. Commun. 0 (2009) 5000.
65. G. Wang, W. Qin, D. Zhang, G. Wei, K. Zheng, L. Wang, F. Ding, J. Fluorine Chem. 130 (2009) 755.
66. L. Xie, Y. Qin, H.-Y. Chen, Anal. Chem. 84 (2012) 1969.
67. F. Zhang, Y. Wan, Y. Shi, B. Tu, D. Zhao, Chem. Mater. 20 (2008) 3778.
68. Y. Q. Lei, H. W. Song, L. M. Yang, L. X. Yu, Z. X. Liu, G. H. Pan, X. Bai, L. B. Fan, J. Chem. Phys. 123 (2005) 174710.
69. J. Yang, Y. Deng, Q. Wu, J. Zhou, H. Bao, Q. Li, F. Zhang, F. Li, B. Tu, D. Zhao, Langmuir 26 (2010) 8850.
70. P. Zou, X. Hong, Y. Ding, Z. Zhang, X. Chu, T. Shaymurat, C. Shao, Y. Liu, J. Phys. Chem. C 116 (2012) 5787.
71. B. Dong, H. W. Song, H. Q. Yu, H. Zhang, R. F. Qin, X. Bai, G. H. Pan, S. Z. Lu, F. Wang, L. B. Fan, Q. L. Dai, J. Phys. Chem. C 112 (2008) 1435.
72. T. H. Ji, F. Yang, H. Y. Du, H. Guo, J. S. Yang, J. Rare Earth. 28 (2010) 529.
73. S. S. Huang, X. J. Kang, Z. Y. Cheng, P. A. Ma, Y. Jia, J. Lin, J. Colloid Interface Sci. 387 (2012) 285.
74. Z. Hou, C. Li, P. Ma, G. Li, Z. Cheng, C. Peng, D. Yang, P. Yang, J. Lin, Adv. Funct. Mater. 21 (2011) 2356.
75. Z. Y. Hou, C. X. Li, P. A. Ma, Z. Y. Cheng, X. J. Li, X. Zhang, Y. L. Dai, D. M. Yang, H. Z. Lian, J. Lin, Adv. Funct. Mater. 22 (2012) 2713.
76. H. P. Paudel, L. Zhong, K. Bayat, M. F. Baroughi, S. Smith, C. Lin, C. Jiang, M. T. Berry, P. S. May, J. Phys. Chem. C 115 (2011) 19028.
77. S. Sivakumar, F. C. J. M. van Veggel, P. S. May, J. Am. Chem. Soc. 129 (2007) 620.
78. W. Que, Y. Zhou, Y. L. Lam, Y. C. Chan, C. H. Kam, L. H. Gan, G. Roshan Deen, J. Electron. Mater. 30 (2001) 7.
79. W. Wu, L. M. Yao, T. S. Yang, R. Y. Yin, F. Y. Li, Y. L. Yu, J. Am. Chem. Soc. 133 (2011) 15810.
80. W. J. Huang, C. H. Lu, C. F. Jiang, W. Wang, J. B. Song, Y. R. Ni, Z. Z. Xu, J. Colloid Interface Sci. 376 (2012) 34.
81. M. L. Yin, L. Wu, Z. H. Li, J. S. Ren, X. G. Qu, Nanoscale 4 (2012) 400.
82. C. Zhang, H. P. Zhou, L. Y. Liao, W. Feng, W. Sun, Z. X. Li, C. H. Xu, C. J. Fang, L. D. Sun, Y. W. Zhang, C. H. Yan, Adv. Mater. 22 (2010) 633.
83. J. C. Boyer, N. J. J. Johnson, F. C. J. M. van Veggel, Chem. Mater. 21 (2009) 2010.
84. R. Xu, J. Li, J. Wang, X. F. Wang, B. Liu, B. X. Wang, X. Y. Luan, X. D. Zhang, Sol. Energy Mater. Sol. Cells 94 (2010) 1157.
85. X. S. Qu, H. W. Song, X. Bai, G. H. Pan, B. Dong, H. F. Zhao, F. Wang, R. F. Qin, Inorg. Chem. 47 (2008) 9654.
86. Z. Yin, Y. S. Zhu, W. Xu, J. Wang, S. Xu, B. Dong, L. Xu, S. Zhang, H. W. Song, Chem. Commun. 49 (2013) 3781.
87. G. Lu, S. Z. Li, Z. Guo, O. K. Farha, B. G. Hauser, X. Y. Qi, Y. Wang, X. Wang, S. Y. Han, X. G. Liu, J. S. DuChene, H. Zhang, Q. C. Zhang, X. D. Chen, J. Ma, S. C. J. Loo, W. D. Wei, Y. H. Yang, J. T. Hupp, F. W. Huo, Nat. Chem. 4 (2012) 310.
88. M. C. Tan, S. D. Patil, R. E. Riman, ACS Appl. Mater. Interfaces 2 (2010) 1884.
89. C. K. Lin, M. T. Berry, R. Anderson, S. Smith, P. S. May, Chem. Mater. 21 (2009) 3406.
90. Y. Li, G. F. Wang, K. Pan, B. J. Jiang, C. G. Tian, W. Zhou, H. G. Fu, J. Mater. Chem. 22 (2012) 20381.
91. L. Ren, X. Qi, Y. D. Liu, Z. Y. Huang, X. L. Wei, J. Li, L. W. Yang, J. X. Zhong, J. Mater. Chem. 22 (2012) 11765.
92. B. M. van der Ende, L. Aarts, A. Meijerink, Phys. Chem. Chem. Phys. 11 (2009) 11081.
93. M. Zhang, Y. J. Lin, T. J. Mullen, W. F. Lin, L. D. Sun, C. H. Yan, T. E. Patten, D. W. Wang, G. Y. Liu, J. Phys. Chem. Lett. 3 (2012) 3188.
94. J. Zhang, H. O. Shen, W. Guo, S. H. Wang, C. T. Zhu, F. Xue, J. F. Hou, H. Q. Su, Z. B. Yuan, J. Power Sources 226 (2013) 47.
95. P. Gibart, F. Auzel, J. C. Guillaume, K. Zahraman, Jpn J. Appl. Phys. 1. 35 (1996) 4401.
96. A. C. Atre, A. Garcia-Etxarri, H. Alaeian, J. A. Dionne, J. Opt. 14 (2012) 024008.
97. G. B. Shan, H. Assaaoudi, G. P. Demopoulos, ACS Appl. Mater. Interfaces 3 (2011) 3239.
98. L. T. Su, S. K. Karuturi, J. S. Luo, L. J. Liu, X. F. Liu, J. Guo, T. C. Sum, R. R. Deng, H. J. Fan, X. G. Liu, A. I. Y. Tok, Adv. Mater. 25 (2013) 1603.
99. J. Zhou, Y. Sun, X. X. Du, L. Q. Xiong, H. Hu, F. Y. Li, Biomaterials 31 (2010) 3287.
100. F. Wang, D. Banerjee, Y. S. Liu, X. Y. Chen, X. G. Liu, Analyst 135 (2010) 1839.
101. M. Lin, Y. Zhao, S. Q. Wang, M. Liu, Z. F. Duan, Y. M. Chen, F. Li, F. Xu, T. J. Lu, Biotechnol. Adv. 30 (2012) 1551.

102. H. Y. Xing, W. B. Bu, S. J. Zhang, X. P. Zheng, M. Li, F. Chen, Q. J. He, L. P. Zhou, W. J. Peng, Y. Q. Hua, J. L. Shi, Biomaterials 33 (2012) 1079.
103. L. Cheng, C. Wang, X. X. Ma, Q. L. Wang, Y. Cheng, H. Wang, Y. G. Li, Z. Liu, Adv. Funct. Mater. 23 (2013) 272.
104. G. Y. Chen, J. Shen, T. Y. Ohulchanskyy, N. J. Patel, A. Kutikov, Z. P. Li, J. Song, R. K. Pandey, H. Agren, P. N. Prasad, G. Han, ACS Nano 6 (2012) 8280.
105. D. J. Naczynski, T. Andelman, D. Pal, S. Chen, R. E. Riman, C. M. Roth, P. V. Moghe, Small 6 (2010) 1631.
106. N. M. Idris, M. K. Gnanasammandhan, J. Zhang, P. C. Ho, R. Mahendran, Y. Zhang, Nat. Med. 18 (2012) 1580.
107. J. N. Shan, S. J. Budijono, G. H. Hu, N. Yao, Y. B. Kang, Y. G. Ju, R. K. Prud'homme, Adv. Funct. Mater. 21 (2011) 2488.
108. L. P. Qian, L. H. Zhou, H. P. Too, G. M. Chow, J. Nanopart. Res. 13 (2011) 499.

Authors

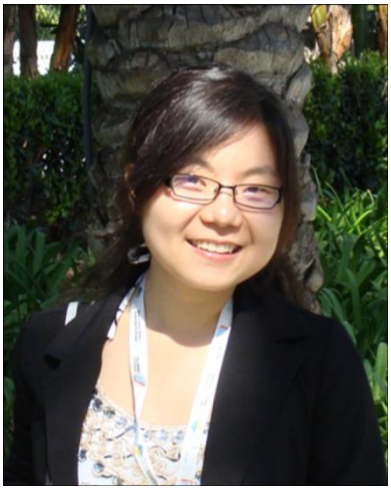

Ying Bao received her Bachelor of Engineering Degree in Pharmaceutical Engineering from Zhejiang Chinese Medical University, China, in 2008. She received her MS Degree in Chemistry in 2010 and her PhD Degree in Material Chemistry in 2013 from the University of South Dakota under the supervision of Prof. Chaoyang Jiang. Dr. Bao has published about ten peer-reviewed articles in various scientific journals, including a recent cover story in *Nanoscale*. Currently she is working at the University of Chicago as a postdoctoral researcher. Her research interest focuses on surface modification, assembly, and optical performance of nanoscale materials for unique applications.

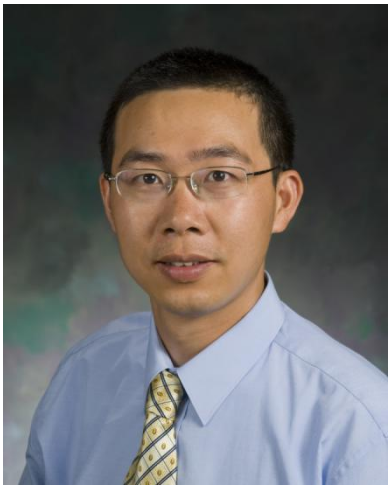

Chaoyang Jiang received the BS Degree in 1996 and the Ph.D. Degree in 2000 from Nanjing University, China. From 2000 to 2007, he had his postdoctoral trainings in Johannes Gutenberg University Mainz, Germany, Iowa State University, and Georgia Institute of Technology. He joined the Department of Chemistry at the University of South Dakota as an Assistant Professor in 2007 and was then promoted to Associate Professor in 2013. Dr. Jiang has published over sixty research papers and review articles in various peer-reviewed scientific journals. His current research interests include layer-by-layer assembly, electrospun nanofibers, metallic and semiconductor nanostructure, upconversion nanocomposite, plasmonic nanomaterials, and surface-enhanced Raman scattering.

Cite this article as:

Ying Bao *et al.*: **Hierarchical upconversion nanocomposite materials containing lanthanide-doped nanoparticles.** *J. Nanosci. Lett.* 2014, **4:** 22